DOI: 10.1021/ma101217y

Macromolecules
ARTICLE

Enthalpy Recovery of PMMA/Silica Nanocomposites

Virginie M. Boucher,*,† Daniele Cangialosi,‡ Angel Alegría,‡,§ and Juan Colmenero†,‡,§

†*Donostia International Physics Center, Paseo Manuel de Lardizabal 4, 20018 San Sebastián, Spain,* ‡*Centro de Física de Materiales Centro Mixto (CSIC-UPV/EHU), Paseo Manuel de Lardizabal 5, 20018 San Sebastián, Spain, and* §*Departamento de Física de Materiales, Universidad del País Vasco (UPV/EHU), Apartado 1072, 20080 San Sebastián, Spain*

Received June 2, 2010; Revised Manuscript Received August 11, 2010

ABSTRACT: In this work, we have studied the effect of silica particles on the physical aging of nanocomposites based on poly(methyl methacrylate) (PMMA). To do that, we have followed the enthalpy relaxation by means of differential scanning calorimetry (DSC). In agreement with previous results carried out by means of broadband dielectric spectroscopy (BDS), we observe an acceleration of the physical aging process of PMMA nanocomposites in comparison to bulk PMMA. The fitting of the enthalpy relaxation results to the well-known Tool−Narayanaswamy−Moynihan (TNM) model gives rise to equal structural parameters for all investigated samples, including bulk PMMA. This implies that the molecular mechanism for physical aging in PMMA is not affected by the presence of silica particles. The only parameter changing is the pre-exponential factor setting the time scale of physical aging. The values obtained are correlated to the area/volume ratio of silica particles in the polymer and thereby to the silica interparticle distance in the nanocomposites. This latter observation is an indication that the physical aging process is driven by the diffusion of free volume holes toward polymer interfaces, as already proposed in the past.

Introduction

Recently, polymer nanocomposites have attracted great attention due to their unique properties (enhanced mechanical strength, thermal stability, or higher chemical resistance etc.) and possibility for numerous applications in modern technology. These unique properties are the result of the combination, or sometimes the synergy, of the physical and chemical properties of inorganic nanoparticles and polymer matrix, and are the main driving force in the research of novel inorganic−polymeric nanocomposites.[1−4]

Whereas numerous aspects of these materials have been extensively studied, from their processing to the characterization of their mechanical and physical properties, the effect of nanoscale fillers on the so-called physical aging behavior of polymer glasses remains relatively uncharted. This aging behavior deals with the slow evolution of thermodynamic properties (enthalpy, volume, etc.) toward equilibrium, occurring below the glass transition temperature (T_g).[5,6] The kinetics of such evolution is intimately related to the molecular mobility in the glassy state.[5,6] Thus, the understanding of physical aging is not only very intriguing from a fundamental point of view, but also of the utmost importance for technological applications of polymer glasses in general. It may result in many deleterious effects ranging from embrittlement to reduction in permeability and dimensional instability. That is the reason why this phenomenon has been extensively studied for bulk polymer systems in the past years.[5]

In the case of polymer nanocomposites and, more generally, nanoscale structured materials such as, for instance, polymer thin films or polymers in nanopores, the physical aging process can be dramatically modified in comparison to the same process in bulk polymers.[7] These peculiarities of physical aging in polymers structured or confined at the nanoscale explain the revival interest of the scientific community in the subject.[8−28]

*Corresponding author. E-mail: sckboucv@.ehu.es. Telephone: +34 943018804.

So far, the studies on the effects of the nanoconfinement on physical aging have reported seemingly contradictory results.[13,16,22−24] Both acceleration and retardation of structural relaxation during physical aging were reported for different types of nanoconfinement and materials, often explained by the nature of interfacial interactions.[12−15] However, the confinement-induced changes on the physical aging process, whether an acceleration or a retardation is observed, cannot always be explained by changes in the overall molecular mobility (and therefore in the T_g). In particular, deviations from the bulk aging rate are observed at length scales of confinement which are by far too large to induce any change in the molecular mobility as a result of either finite size[29−32] or interfacial effects.[33,34]

As far as polymer thin films with thicknesses of the order of several hundreds nanometers are concerned, the acceleration of physical aging in comparison to the bulk polymer has been explained invoking a mechanism based on the diffusion of free volume holes and their annihilation at the external surface.[21,35−39] Concerning polymer nanocomposites, in a previous work,[40] the physical aging of PMMA—monitored by following the time dependence of the β-process dielectric relaxation strength by means of broadband dielectric spectroscopy (BDS)—was shown to be accelerated in PMMA/silica nanocomposites in comparison to the bulk, despite the lack of effect of silica particles on PMMA segmental dynamics. In ref 40, the diffusion of free volume holes model accurately described the time-dependence of the dielectric relaxation strength measured on the investigated samples. Moreover, the dependence of the physical aging rate on the ratio area of silica/volume of PMMA—in the investigated nanocomposites—was put in evidence. These results indicated that physical aging in polymer nanocomposites, as in other nanostructured polymer systems, seems to be compatible with the mechanism of diffusion of free volume holes toward the interfaces between the polymer and the nanoparticles.

In the present work, our previous results are confirmed by means of differential scanning calorimetry (DSC), which directly

 Published on Web 08/26/2010

Table 1. Summary of PMMA and PMMA Nanocomposites Characteristics: Silica Weight Fraction, Particles Surface-Treatment, Silica Particles Diameter, Interparticle Distance, PMMA Glass Transition Temperature, and Total Recovered Enthalpy

sample	silica weight fraction, W_f (%)	surface treatment	particles diameter (nm)	interparticle distance, l (nm)	T_g (°C)	$\Delta H_{plateau}$ (J.g^{-1})
PMMA					123.4	2.1
A10	8.9	TPM	350	1410	123.0	1.95
R10	8.9	OTMS	350	1410	122.5	1.9
V10	8.9	TPM	200	806	123.4	1.85

follows the evolution of the enthalpy, i.e., an actual thermodynamic magnitude. The results of this study also showed an acceleration of the physical aging of PMMA in the presence of silica nanoparticles. In order to allow the quantitative comparison and the physical interpretation of the results, the kinetics of the physical aging process as determined from DSC experiments have been fitted by means of the Tool−Narayanaswamy−Moynihan (TNM) phenomenological model. The equality, for all the samples, of the structural fitting parameters set to achieve a good modeling of the results through the TNM model led us to the conclusion that the acceleration of the physical aging of PMMA in the composite samples is not related to a modification of the molecular mechanism involved in the aging process. Rather, the modeling of the results highlighted a correlation between the physical aging rates and the ratio area of silica/volume of polymer. The observation that a higher ratio area of silica/volume of PMMA gives rise to a higher physical aging rate—at least for the investigated samples—reinforced the idea that, in polymer nanocomposites, physical aging process is driven by the diffusion of free volume holes to the polymer interfaces.

In the following, we first provide a summary of the experimental methods and results, then present the modeling of the enthalpy recovery data to TNM phenomenological model, and finally apply the diffusion of free volume holes model to these enthalpy recovery data.

Experimental Section

Preparation of the Pure Polymer and Polymer Nanocomposites. Silica particles with diameters of 200 and 350 nm were prepared as described elsewhere using a variation of the Stöber method.[41] Surface modification was carried out for hydrophobation of silica surfaces using silane coupling agents. Thus, 350 nm silica particles were functionalized using two different silane coupling agents: 3-(trimethoxysilyl)propyl methacrylate (TPM), and octadecyltrimethoxysilane (OTMS). In the case of particles with a diameter of 200 nm, only TPM was employed as surface modifier.

Briefly, the final samples were prepared by in situ polymerization of methyl methacrylate (MMA) in presence of the photoinitiator DMPA (2,2-dimethoxy-2-phenylacetone) and the previously described silica particles. The detailed preparation of PMMA and PMMA/silica nanocomposite samples is described in a previous paper.[41] The so-obtained materials are listed in Table 1.

Characterization of the Samples. The weight fraction of silica particles in the nanocomposite samples was measured by thermogravimetric analyses (TGA), on a thermogravimeter TA Q-500, with a heating ramp of 10 °C·min^{-1} up to 750 °C under flowing nitrogen (20 cm^3·min^{-1}). The values of silica weight fraction are reported in Table 1.

Thermal analyses of the samples were carried out by means of the differential scanning calorimeter (DSC) (DSC-Q2000 from TA-Instruments). The temperature was calibrated with melting indium. All DSC measurements were performed under nitrogen atmosphere on samples of about 10 mg. Hermetic aluminum pans were used for all the materials. For the study of physical aging, all experiments began with a heating ramp to a temperature of 150 °C in order to erase the material's previous thermal history. The samples were subsequently cooled down at a programmed rate of 20 °C·min^{-1} to reach 40 °C before being stabilized at the temperature used for structural recovery (80 °C), aged in the calorimeter for times from several minutes to 16 h before being cooled to 40 °C at a cooling rate of 20 °C·min^{-1}, prior to reheating at 10 °C·min^{-1} (see Figure 1). For the measurements of the enthalpy relaxation at longer aging times ($t_a \geq 24$ h), the annealing of the samples was carried out in an external vacuum oven, at a temperature of 80 °C, after erasing of the thermal history and quenching of the samples in DSC. After aging, the samples were quenched again and DSC thermograms were recorded. Second scans were performed immediately after a new quench at 20 °C·min^{-1}. In the case of the sample V10, the physical aging process was monitored also at the following annealing temperatures: 77, 83, and 90 °C.

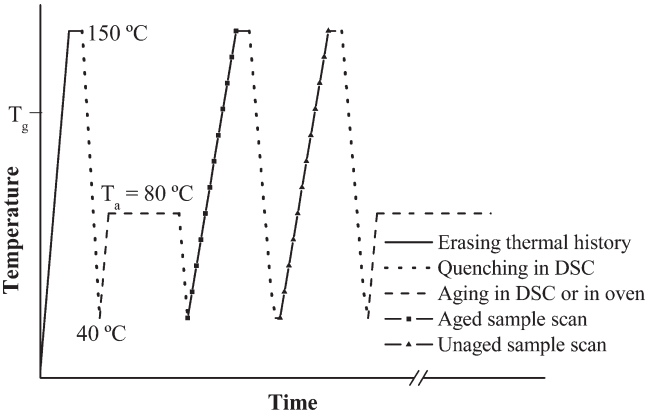

Figure 1. Thermal history for enthalpy relaxation measurements.

As a general procedure in calorimetric experiments, the amount of enthalpy relaxed during aging (and thus recovered during DSC scan) of a glass for a period of time t_a at a given temperature T_a was evaluated by integration of the difference between thermograms of aged and unaged samples, according to the relation:[42]

$$\Delta H(T_a, t_a) = \int_{T_x}^{T_y} (C_p^a(T) - C_p^u(T))\, dT \qquad (1)$$

In this equation, $C_p{}^a(T)$ and $C_p{}^u(T)$ are the heat capacities measured respectively after annealing and on the unannealed sample, respectively, whereas T_x and T_y are reference temperatures ($T_x < T_g < T_y$). On the other hand, eq 1 actually provides the expression of the experimental enthalpy difference between the thermal treatments with and without annealing at a temperature set at 80 °C in this work.

Results

Microscopy and Dynamics of Pure Polymer and Nanocomposites. In this section, we summarize the results previously obtained by us for all nanocomposites and pure PMMA[40] with particular attention to the dispersion of silica nanoparticles in PMMA and the effect of the nanoparticles on PMMA segmental dynamics.

TEM micrographs of all investigated PMMA/silica nanocomposites, presented in our previous paper,[40] showed a very good dispersion of the silica particles in the samples A10 and V10. In the sample R10, the dispersion of silica particles is

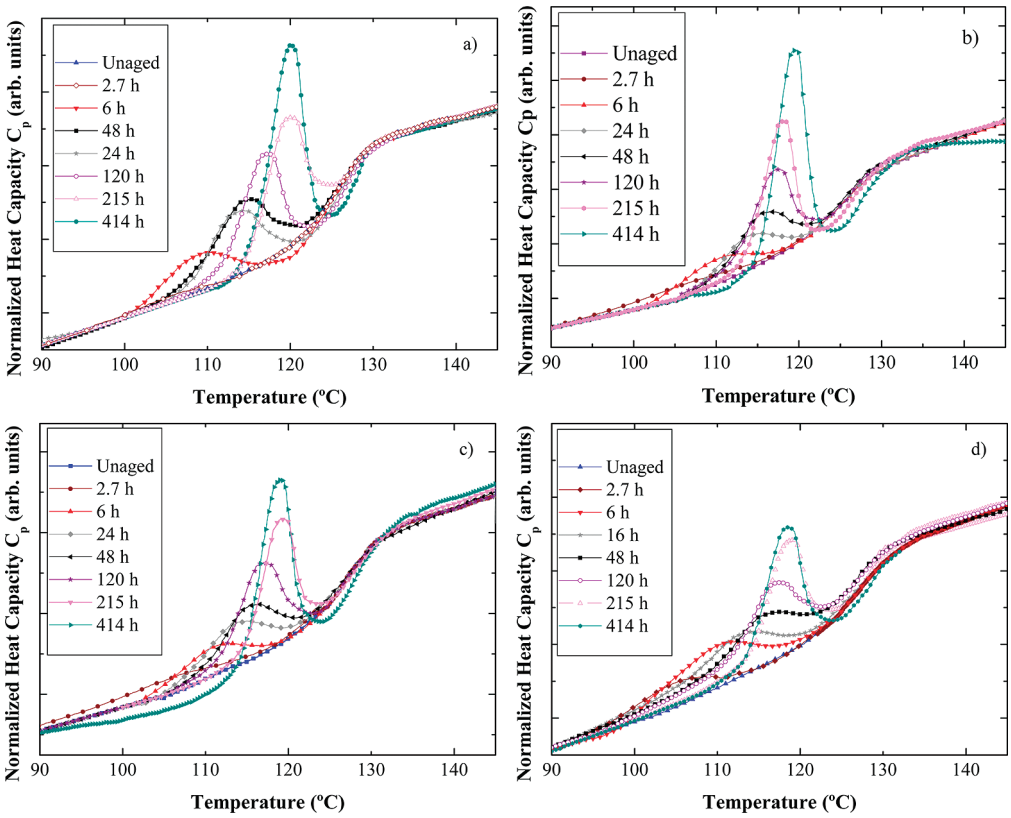

Figure 2. DSC scans of the heat capacity versus temperatures for (a) PMMA, (b) A10, (c) R10, and (d) V10, after isothermal annealing at 80 °C for various aging times.

not as homogeneous as in the other composite samples. Nonetheless, it is important to notice that in the sample R10 the silica particles are not aggregated, which means that the ratio area of silica/volume of PMMA is not affected by this uneven dispersion. These observations show that both surface treatments of the silica particles (TPM and OTMS) are effective in the prevention of particles aggregation, in particular the surface treatment with TPM. Furthermore, the TEM images of PMMA nanocomposites allow checking that the average interparticle distance of silica in the different samples corresponds to the expected one from geometrical arguments, reported in Table 1.

The values of the T_g(s) recorded by means of DSC, at 10 °C·min^{-1}, on cooling, for pure PMMA and the three investigated nanocomposites, are reported in Table 1. For all the samples, the addition of silica does not affect the position of the glass transition. This result is corroborated by recently published results on the molecular dynamics of PMMA/silica nanocomposites detected by BDS.[40] These actually show that PMMA glassy dynamics does not depend on the presence of nanoparticles or on the surface-treatment of the particles, both above and below the T_g, in the case of the investigated samples. These results are consistent with previously published literature data also displaying no shift in the T_g of PMMA in PMMA/silica nanocomposites (or PMMA thin films supported on silica) with typical interparticle distances (or thicknesses) larger than 100 nm.[12,13,43−45] For PMMA/silica nanocomposite systems presenting interparticle distances—or thicknesses for PMMA thin films supported on silica—smaller than 100 nm, the glass transition behavior is still a matter of open debate: while some authors report a significant increase of the T_g,[12,13,43] others studies do not observe any shift in the T_g.[44,45]

Enthalpy Recovery. In DSC experiments, the structural recovery that occurs with increasing annealing times is observed experimentally as the development of an endothermic overshoot in the DSC thermogram. Isothermal structural recovery or physical aging results in larger overshoots and lower "fictive temperature, T_f,"[46] as aging time increases. Figure 2 shows the DSC heating scans after various aging times for PMMA and for the nanocomposite samples, for the aging temperature, T_a, of 80 °C (43 °C below the nominal T_g). For ease of comparison, we plot the normalized heat capacity, C_p, i.e. the heat capacity of the sample after the removal of the contribution from silica and normalization to the exact mass of PMMA in the sample. To do so, the temperature dependence of silica heat capacity was calculated and deduced from the total heat capacity of the sample, according to the silica weight fraction in the nanocomposite sample. As aging time increases, the magnitude of the endothermic overshoot increases, as well as the temperature of its maximum, T_p, as expected. A common feature of the calorimetric plots of all investigated samples is the fact that the endothermic overshoot shows up as a "pre-peak" followed, at higher temperature, by a minimum in the specific heat. This result is in agreement with those found by others in PMMA.[47−51]

However, the nanocomposite sample V10 shows smaller and broader overshoots than the ones of the bulk polymer for aging times $t_a > 6$ h. The interesting feature of Figure 2d is that for the shortest aging times (2.7 and 6 h), the nanocomposite sample scans exhibit significantly more important endothermic overshoots. The endothermic overshoot of the nanocomposite appears to develop for shorter aging times than the neat polymer, and to reach a plateau in the time scale of 414 h, whereas PMMA sample displays a continuous increase of its endothermic overshoot. Similar observations were made on the thermograms of the nanocomposite samples A10 and R10 (Figure 2, parts b and c),

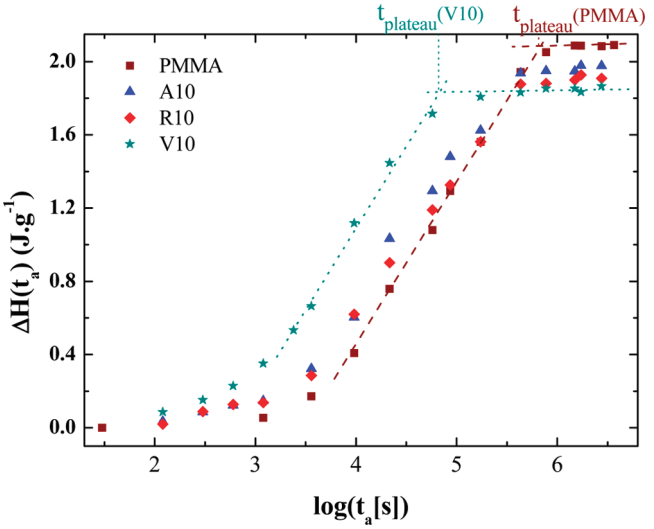

Figure 3. Relaxed enthalpy versus log aging time, for PMMA, and its nanocomposites. All values are normalized to the weight of PMMA. The dotted (···) and dashed (- - -) lines correspond to the geometrical construction applied to determine the time to reach the plateau, respectively, for V10 and pure PMMA, as examples.

obtained after annealing: for the same aging time, the magnitude of the overshoot of both samples was found to be equivalent for the two samples, and to be intermediate between that of PMMA and that of V10. Moreover, the aging time required to reach the final structural state in the case of the samples A10 and R10 appeared to be comprised between the respective aging times needed for PMMA and V10 samples. These qualitative observations are confirmed by the calculation of the amount of relaxed enthalpy, $\Delta H(t_a)$, after aging at 80 °C for various aging times, through eq 1. In Figure 3, where the so-calculated values of $\Delta H(t_a)$ are plotted versus aging time, one can observe that for short aging times ($t_a \leq 6$ h) the amount of relaxed enthalpy is larger for the nanocomposite samples in comparison with bulk PMMA. Then the values of $\Delta H(t_a)$ for the nanocomposite samples get slightly smaller than that of neat PMMA as the nanocomposite samples reach a final structural state, characterized by a plateau appearing at shorter aging times than that required by the bulk PMMA sample. This result will be discussed in details in the Discussion.

The values of the total recovered enthalpy, $\Delta H_{plateau}$, calculated from the plots of the specific heat versus temperature, are reported in Table 1. It is worth noticing that the value of $\Delta H_{plateau}$ is significantly smaller (accounting for about 20%) than that obtained extrapolating the enthalpy from the liquid state. This result is consistent with others presented in the past.[52−56] In this respect, it should be pointed out that a realistic experimental estimation of $\Delta H(\infty)$ is possible only in a very narrow temperature interval below T_g, whereas alternative approaches on the basis of empirical procedures[54,57] are questionable. However, these findings could depend on the failure of the excess of thermodynamic variables in approaching the value extrapolated from the melt at long aging times. This possibility has been recently proposed by Pyda and Wunderlich,[58] who—assessing the different contributions to the specific heat of melt polyethylene—concluded that the mere extrapolation of thermodynamic properties below the T_g underestimates the actual values of those properties. This implies that the extrapolation of the melt behavior does not provide the limit of the thermodynamic values observable in the glass. In Figure 4, we schematically highlight the difference between the enthalpy experimentally recovered and the

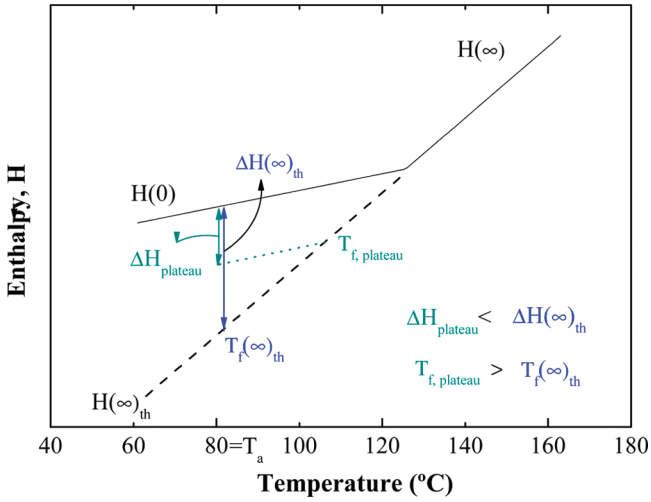

Figure 4. Schematic illustration of the discrepancy between the theoretical equilibrium value of the recovered enthalpy, $\Delta H(\infty)_{th}$,and the experimental plateau value, $\Delta H_{plateau}$. The different fictive temperatures $T_f(\infty)_{th}$ and $T_{f,\,plateau}$—corresponding respectively to the different values of recovered enthalpy $\Delta H(\infty)_{th}$, and $\Delta H_{plateau}$—are also represented.

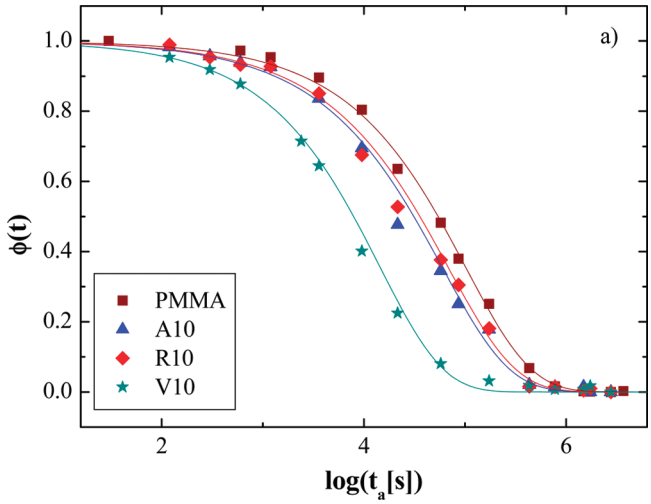

Figure 5. Structural relaxation function $\phi(t)$ for T_a = 80 °C, for all investigated systems. Continuous lines correspond to the fits to the TNM model.

enthalpy obtained by merely extrapolating this variable from the melt. Whatever the possible evolution of the enthalpy for longer aging times—which is not the subject of our investigation—Figure 3 indicates that a plateau in the recovered enthalpy is achieved in the time scale of our aging experiments. As far as the enthalpy recovered by the nanocomposites is concerned, it is generally slightly smaller than that recovered by pure PMMA. This result will be discussed in details in the Discussion.

In Figure 5, the experimental data concerning the enthalpy relaxation of PMMA and the nanocomposite samples at the aging temperature of 80 °C are reported as a function of the aging time. The data are reported as normalized relaxation isotherms, defined by the widely used function describing enthalpy relaxation of glasses:[59,60]

$$\phi(t_a) = \frac{\Delta H(t_a) - \Delta H_{plateau}}{\Delta H(0) - \Delta H_{plateau}} \qquad (2)$$

where $\Delta H(t_a)$ was evaluated according to eq 1; $\Delta H(0)$, the value of the enthalpy at zero aging time was taken equal to

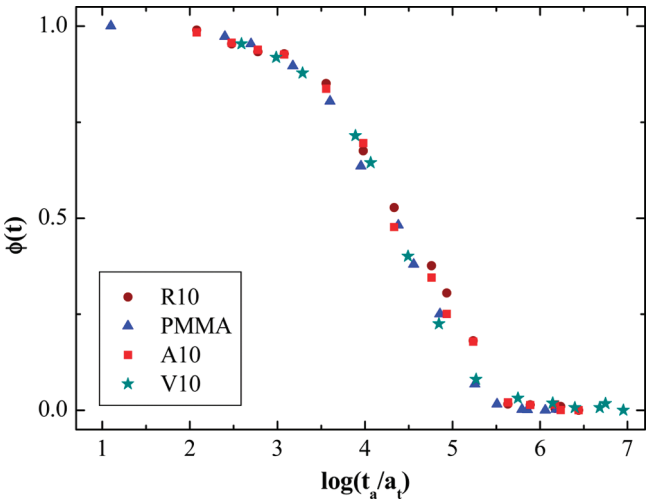

Figure 6. Superposition of the relaxation functions of all nanocomposites and pure PMMA, after shifting the time scale of the shift factor a_t. The nanocomposites A10 and R10 are taken as the reference.

zero; $\Delta H_{plateau}$, the asymptotic value of the recovered enthalpy at the selected aging temperature T_a, was obtained through eq 1 for the largest aging times, at which the recovered enthalpy reaches a plateau.

The so-defined relaxation function is an appropriate mathematical tool to quantitatively study physical aging, since it takes into account the thermodynamic driving forces for aging. This is actually defined by the quantity $\Delta H(0) - \Delta H_{\text{plateau}}$. Thus, the relaxation function $\phi(t)$ allows a nonambiguous definition of the physical aging rate for those systems displaying different thermodynamic driving forces or for the same system at different aging temperatures.

The plots displayed in Figure 5—with the value of $\Delta H_{plateau}$—confirm the fact that bulk PMMA and PMMA nanocomposites exhibit different physical aging behaviors. The significantly accelerated physical aging of the nanocomposite sample V10 in comparison to the bulk sample is well illustrated in Figure 5 that clearly shows that V10 relaxation function reaches a plateau at aging times shorter than the other samples. Here, it is worth remarking that the rate of physical aging is defined as the *absolute* time scale to reach the plateau in the relaxation function, rather than defined as the slope of the relaxation function vs time plots in some specific point. These results are consistent with the acceleration of physical aging observed when comparing the magnitude of endothermic overshoots in PMMA and V10 thermograms obtained after different aging times, in particular for the shortest aging times (see Figure 2).

For the other nanocomposite samples, A10 and R10, the increase in the physical aging rate in comparison to the bulk sample is also evident in Figure 5, even if less pronounced than for the sample V10. Another interesting feature of Figure 5 is the fact that R10 and A10 display the same physical aging behavior, suggesting that the physical aging is independent of the surface-treatment of the silica particles, for the samples investigated in this work. Furthermore, it is worth noticing that previous work on PMMA/silica nanocomposites[44] indicates that the interaction between the silica surface and the polymer extends up to a couple of nm from the interface silica/polymer. This means that—considering that our samples present typical interparticle distances of the order of 1 μm—the effect of silica/polymer interaction on the physical aging phenomenon is expected to be negligible (affecting less than 1% of the polymer), in the investigated samples. As the studied samples differ only from the area/volume ratio of silica in the polymer matrix, apart from A10 and R10 which present the same area/volume ratio of silica, it appears that the physical aging rates of PMMA in the nanocomposite samples depend on this parameter, as has already been pointed out in our previous work.[40] The higher is the area/volume ratio of silica in PMMA, the faster is the physical aging of PMMA. Although this conclusion is achieved only for two different area/volume ratios of silica, it is important to remark that (i) the sample with the largest ratio (V10) presents the largest rate of physical aging and (ii) samples with identical ratios (A10 and R10) display identical rates of physical aging. Furthermore, very recent results on similar nanocomposite systems presenting a much wider range of silica concentrations fully confirm the conclusion of increasing rate of physical aging with increasing the area/volume ratio of silica.[61] In the latter case, area/volume ratios corresponding to typical interparticle distances of the order of 100 nm were achieved. It was observed that this increase in the area/volume ratio to reach interparticle distances of the order of 100 nm led to a 2 orders of magnitude decrease in the time to reach the plateau for these systems in comparison with bulk PMMA.

It is interesting to notice that the relaxation curves of all nanocomposites and pure PMMA can be superimposed on a master curve by mere horizontal shifting,[62] as displayed in Figure 6. This result suggests that the underlying molecular mechanism for physical aging is not affected by the presence of silica nanoparticles. Further analysis by the TNM model, presented and discussed in details in the next section of the paper, corroborates this hypothesis. As far as the present discussion is concerned, the superposition of all relaxation functions onto a master curve implies that the characteristic time for physical aging can be expressed as

$$\tau_{PA} = \tau_{SR} \cdot f_{A/V} \tag{3}$$

where τ_{SR} is the structural relaxation time, equivalent for all the investigated samples and thus related to the intrinsic molecular mobility; and $f_{A/V}$ is a factor that accounts for the difference in the rate of physical aging among the samples. Thus, $f_{A/V}$ accounts for the horizontal shift needed to superimpose the relaxation functions of all nanocomposites and pure PMMA (see Figure 6). Considering that the nanocomposites differ from pure PMMA for the area of silica to volume of PMMA ratio, we speculate that $f_{A/V}$ accounts for the contribution of such a ratio in determining the physical aging rate.

To conclude this section, the following results can be highlighted: (i) PMMA and PMMA/silica nanocomposites display the same segmental glassy dynamics (ii) the nanocomposite samples exhibit accelerated physical aging in comparison to bulk PMMA (iii) the rate of physical aging seems to be closely related to the area/volume ratio of silica in PMMA.

Models Development

TNM Model. To get further insight on the actual importance of the area/volume ratio of silica on the physical aging of PMMA in the different samples, we have analyzed our data in the light of the TNM model habitually used for the characterization of the enthalpy relaxation behavior of polymers. Since the physical aging behavior of PMMA nanocomposites differs from that of pure PMMA, the sensitivity of the model parameters to the presence of silica particles in PMMA, and in particular to the changes in the area/volume ratio of silica in the PMMA matrix, will be examined.

The TNM model is based on some fundamental assumptions[42] intimately related to the peculiar nature of the glassy state. To consider the nonexponential character of relaxation in glass-forming systems, the stretched exponential function:

$$\phi(t) = \exp\left[-\left(\frac{t}{\tau_{PA}}\right)^{\beta}\right] \quad (4)$$

is used to describe the relaxation function (eq 2), where the shape parameter β is assumed to be constant by invoking the time−temperature superposition principle.[62] Here, τ_{PA} refers to the relaxation time associated with the physical aging process (see eq 3). A second basic feature of the structural relaxation of glasses is its nonlinear character attributable to the out-of-equilibrium nature of the glassy state. During aging, the structure of the system changes, providing a self-retarding relaxation mechanism. Several expressions were proposed to describe the nonlinear character of physical aging. Phenomenological models of the glass transition such as the TNM[52,60,63,64] and Kovacs−Aklonis−Hutchinson Ramos (KAHR)[6] models have been found to provide a good description of enthalpy relaxation in a variety of glass formers.[6,9,65−72] In particular, the TNM model expresses the dependence on the structure and the temperature of the relaxation time as:

$$\ln \tau_{PA} = \ln A_{\mathrm{TNM}} + \frac{x\Delta h}{RT} + \frac{(1-x)\Delta h}{RT_f} \quad (5)$$

where $\ln A_{\mathrm{TNM}}$ is a constant, $\Delta h/R$ is the apparent activation energy in the temperature range of the experiment, and x is the nonlinearity parameter which partitions the dependence of τ_{PA} on temperature and structure, the latter of which is quantified by the fictive temperature T_f.[6,52,42,60,64−66,73,74] T_f is determined by Moynihan et al.'s method[52] as the intersection of the extrapolated liquid and glass enthalpy lines through the relation:

$$\int_{T_f}^{T>T_g} (C_{pl} - C_{pg})\, \mathrm{d}T = \int_{T<T_g}^{T>T_g} (C_p - C_{pg})\, \mathrm{d}T \quad (6)$$

where C_{pg} and C_{pl} represent the values of the glassy and liquid heat capacities, respectively. T_f actually provides the structural parameter to the model. It is important to remark that a key feature of this approach is that the parameters (A_{TNM}, x, Δh, β) are material specific parameters. Consequently, they are supposed to describe all the possible experiments, independently of the specific thermal history adopted.

According to the definition of the fictive temperature, it is obtained that the maximum amount of enthalpy releasable at a given temperature, $T_a < T_g$, may be approximately evaluated by the expression:[42,52]

$$\Delta H(T_a, \infty) \approx \Delta C_p(T_g)(T_g - T_{f\infty}) \quad (7)$$

where $T_{f\infty}$ is the fictive temperature corresponding to the maximum recovered enthalpy (see Figure 4). As discussed in the previous section of the paper, this differs from the annealing temperature T_a due to the inability of the enthalpy to recover the value extrapolated from the melt.

In order to reduce the number of fitting parameters, the apparent activation energy, $\Delta h/R$, was evaluated through a shifting procedure, based on the time−temperature superposition principle, which usually provides a reasonable approximation of $\Delta h/R$.[70] To do so, the enthalpy recovery was measured after annealing at various aging temperatures in a temperature range around 80 °C. The results of these experiments are displayed in Figure 7a for the nanocomposite V10, where the typical enthalpy relaxation behavior can be observed, namely a speeding up of the enthalpy relaxation as aging temperature increases. Figure 7b shows the result of shifting the enthalpy data horizontally to the reference temperature of 77 °C in such a way that the data superimpose on a wide range of times. Here data coincide very well to a reduced curve on the experimental time range. The logarithm of the shift factors, a_T, used to shift the enthalpy data are shown in the inset of Figure 7b, as a function of the inverse of temperature. This plot confirms that the time−temperature superposition principle can be applied since the shift factors display an Arrhenius dependence to temperature, from which the apparent activation energy for enthalpy relaxation, Δh, can be estimated to be 213 kJ mol^{-1}. As will be shown later in the paper, this value of Δh, determined for the nanocomposite sample V10 for convenience,[75] can be used to describe the enthalpy relaxation data according to the TNM model for all investigated samples. One can observe a difference in this value of Δh in comparison to that published by Hodge,[66,76] reporting a significantly larger value. Nevertheless, this discrepancy between the value of Δh determined in our work and that provided by Hodge[66,76] for

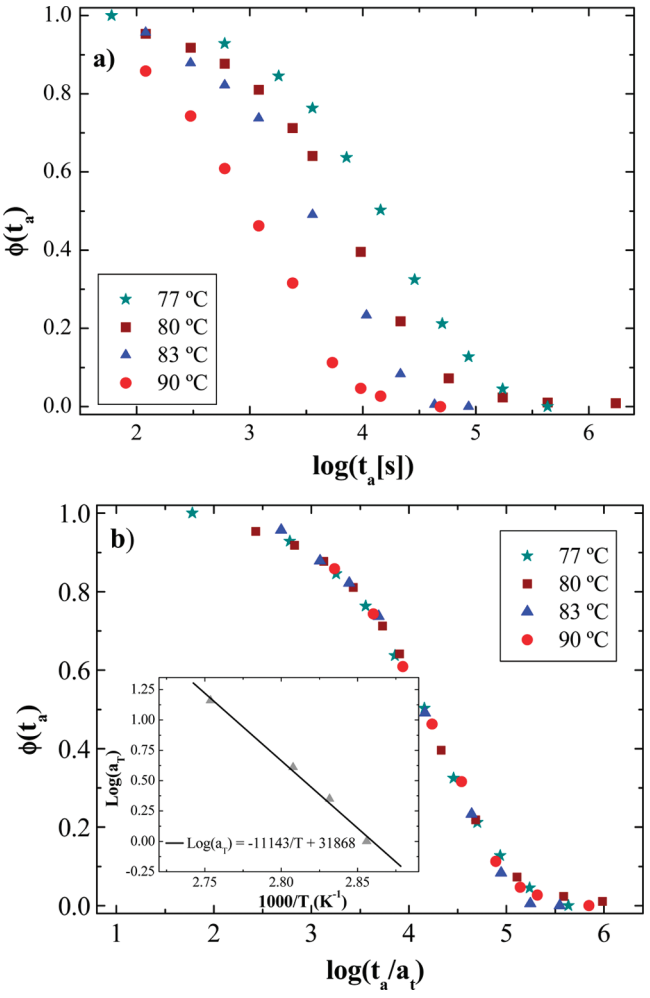

Figure 7. (a) Evolution of the enthalpy relaxation function with aging time, for various annealing temperatures, for the nanocomposite sample V10. (b) Time−temperature superposition of enthalpy relaxation function versus time curves, for the nanocomposite sample V10, after shifting the time-scale of the shift factor a_i; The inset to part b displays the temperature dependence of the shift factors used to superimpose the isothermal enthalpy relaxation functions.

Table 2. Best Fit Parameters and Mean Square Error (MSE) Obtained from the Fit of Enthalpy Relaxation Data to the TNM Model, with $\Delta h = 213$ kJ mol^{-1}

sample	area to volume ratio A/V (nm^{-1})	A_{TNM} (s)	β	x	*MSE*
PMMA		5.40×10^{-26}	0.58	0.36	0.0043
A10	8.0×10^{-4}	3.03×10^{-26}	0.58	0.36	0.0092
R10	8.0×10^{-4}	3.28×10^{-26}	0.58	0.36	0.0095
V10	1.4×10^{-3}	5.81×10^{-27}	0.59	0.37	0.0038

PMMA has to be discussed carefully. An important factor which has to be highlighted in Hodge's work[66,76] is the fact that the value of Δh was determined from the cooling rate dependence of the fictive temperature in a temperature range very close to T_g. In other words, this value of Δh corresponds to the activation energy of the α relaxation. In our study, Δh results from the shifting procedure of structural relaxation data measured after annealing in a range of temperatures significantly lower than T_g (77 °C ≤ T_a ≤ 90 °C), in which the physical aging process may be driven by a different molecular mechanism. In this case, Δh is comprised between the respective activation energy values of PMMA α and β process. This result is consistent with those found by other authors studying physical aging of different glasses, including our previous study by BDS.[40,77−80]

Thus, the fitting to the TNM model was performed by optimizing the values of x, β, and A_{TNM}, after having imposed the predetermined value of Δh. A mean square error minimization procedure was adopted. The optimized parameters of the TNM model are reported in Table 2. Only small variations of β and x appeared, whereas significant differences of the ln A_{TNM} can be observed among the samples. In Figure 5, the fits to the TNM model are displayed as continuous lines for each set of data. As can be observed, the TNM model describes rather well the enthalpy relaxation function for bulk PMMA and PMMA nanocomposites. The fitting results obtained for PMMA can be compared to those reported in the literature.[66,76] On one hand, the correlation between β and x, and the one between Δh and x are in agreement with the empirical correlations proposed by Hodge.[76] On the other hand, a significant difference appears in the absolute values of these parameters in comparison with those published by Hodge in a previous paper:[66] the values of β, x, and A_{TNM} reported in his work are by far lower than that resulting from the fit of our data, which is not surprising considering that the imposed values of Δh are significantly different in the two studies, as previously commented.

Within the scope of the present study, more interesting is the comparison of the values of the fitting parameters obtained for bulk PMMA and PMMA/nanocomposites. The structural parameters, β, x, and Δh of the TNM model were found to be equal for all the studied samples. This observation provides good evidence that the molecular mechanism involved in the physical aging of PMMA is not affected by the presence of silica particles in the polymer. This result is in agreement with the invariance of the segmental dynamics as probed by BDS and DSC.[40]

On the other hand, it is important to highlight that the difference in the physical aging rate of PMMA in the different samples is accounted for only by the variation of the pre-exponential factors, A_{TNM}. This result strongly suggests that this pre-exponential factor is intimately related to $f_{A/V}$ of eq 3, namely the parameter accounting for the area of silica to volume of polymer ratio.

Diffusion Model. In previous sections, we have presented experimental data on the dynamics and the physical aging of PMMA/silica nanocomposites and pure PMMA. Furthermore, we have applied the TNM model to describe the enthalpy relaxation data of all systems. Our results can be summarized as follows: (i) PMMA molecular mobility is not affected by the presence of silica nanoparticles; (ii) the equality of the TNM structural parameters (apart from the pre-exponential factor) for the different samples gives evidence that the molecular mechanism responsible for the physical aging of PMMA is the same in the bulk and in PMMA/silica nanocomposites; (iii) a correlation between the physical aging rate and the area/volume ratio of silica in PMMA can be established. These results are compatible with the hypothesis that—in the investigated temperature range—physical aging is driven by the diffusion of free volume holes and their disappearance at a boundary surface[20,21,37−40] (the interface particles/polymer in the case of the nanocomposites; the interface polymer/air in the case of bulk PMMA). The soundness of the diffusion model has been already tested for the physical aging results obtained on the same PMMA/silica nanocomposites by means of BDS, a somehow indirect method.[40] Here we recall the main ingredients of the diffusion model with particular attention to its application to our enthalpy relaxation data. Within this framework, the diffusion of free volume can be expressed by the second equation of Fick:

$$\frac{\partial f_v}{\partial t} = \nabla(D\nabla f_v) \tag{8}$$

where f_v is the free volume fraction and D is the diffusion coefficient. Assuming a constant D for short aging times, at which the self-retardation[5] effect has not yet induced a significant decrease of D, eq 8 can be expanded and rearranged to give an expression of the total number of free volume holes at time t, $N(t)$:

$$\frac{N(t)}{N(0)} \approx 1 - \frac{2}{\pi^{0.5}} \frac{A}{V} D^{0.5} t^{0.5} \tag{9}$$

where $N(t)$ equals the integral over the sample volume of the free volume, A is the total surface where free volume holes disappear, V is the total volume, D is the diffusion coefficient at zero aging time, t is the aging time, and $N(0)$ is the number of holes at initial aging time.

The structural relaxation function $\phi(t)$ can be introduced in eq 9, if we consider that the variation of the free volume holes number $N(t)$ is proportionally linked to the variation of the relaxation enthalpy at least for aging times close to zero:

$$\phi(t) \approx 1 - \frac{2}{\pi^{0.5}} \frac{A}{V} D^{0.5} t^{0.5} \tag{10}$$

It is interesting to notice that from a mathematical point of view, eq 10 is equivalent to the stretched exponential of KWW model (see eq 4). In fact, if the stretched exponential is expanded through a Taylor series around zero aging time, an expression analogous to eq 10 is obtained, provided that the stretched exponent equals 0.5.

The diffusion coefficient at the beginning of the aging process can be calculated from the slope of the tangent to the plots of $\phi(t)$ versus $t^{0.5}$ at the shortest aging times, as illustrated in Figure 8, provided that the area to volume ratio, A/V, is known. Indeed, the differentiation of eq 10 with respect to the square root of the time at $t = 0$, gives:

$$\left.\frac{\partial \phi(t)}{\partial t^{0.5}}\right|_{t\approx 0} \approx -\frac{2}{\pi^{0.5}} \frac{A}{V} D^{0.5} \tag{11}$$

where A/V corresponds to the area to volume ratio of silica in PMMA, in the case of PMMA/silica nanocomposites.

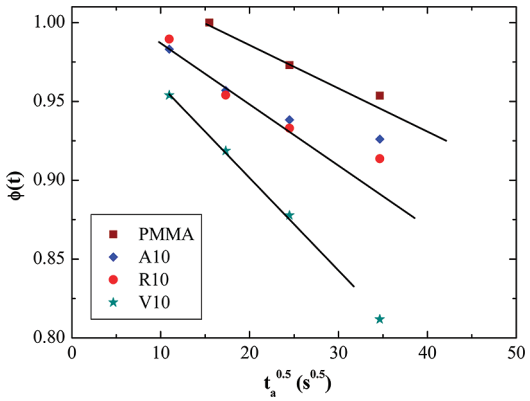

Figure 8. Enthalpy relaxation function $\phi(t)$ with the square root of the aging time for the different samples. The continuous lines represent the tangents to the curves at zero aging time.

For pure PMMA, as described in a previous work,[40] the value of A/V arises from the presence of an internal length that is assumed to be present to fit the physical aging results to the diffusion model with a diffusion coefficient comparable to that of nanocomposites.

The so-obtained diffusion coefficients are given in Table 3, together with the values obtained monitoring the physical aging of the same systems by means of BDS at 80 °C. The latter values differ from those presented in ref 40, since in that case the dielectric strength of PMMA β process at infinite time was taken as the extrapolation of the melt dielectric strength to the selected aging temperature. This led to an underestimation of the decrease of the related relaxation function during physical aging. Thus, similarly to the relaxation function of enthalpy recovery, the values of the diffusion coefficient from BDS reported in Table 3 are calculated considering that the total recovered dielectric strength is of about 20% of the one extrapolated from the melt.

Discussion

The enthalpy relaxation study of PMMA and PMMA/silica composites—as well as the previous BDS study—indicated accelerated structural recovery of PMMA in presence of silica particles, in comparison with bulk systems. This result appears to be in contradiction with most of the studies of the physical aging behavior of polymer nanocomposites, reporting a reduction or even a suppression of physical aging in glassy polymers containing inorganic fillers. While the enthalpy relaxation of an epoxy−clay nanocomposite was shown to be reduced by a factor of 4 with the incorporation of 10 wt % of clay compared to the neat epoxy,[14,19] the physical aging of PMMA[12,13,81] and poly(2-vinylpyridine)[13,81] was found to be suppressed in the presence of silica particles, reduced for PS containing the same silica particles[13] and reduced for PMMA containing single wall carbon nanotubes (SWCNT).[82] In the case of epoxy/clay nanocomposites[19] as for the case of PMMA/SWCNT nanocomposites,[82] the reduction in the enthalpy relaxation rate was rationalized assuming a layer with reduced mobility at the organic−inorganic interface. In the study of PMMA, PS, and PVAc containing silica particles,[12,13,81] the results were explained in the light of the strength of the interactions existing between the inorganic particles and the respective polymers, attractive particles leading to the suppression of the physical aging, through a reduction of the polymer segmental mobility near or at the filler interface. The same explanation was also proposed by Amanuel et al.[15] studying the physical aging behavior of poly(vinyl acetate) (PVAc)/silica nanocomposites displaying an apparent reduced physical aging rate in comparison to the bulk. In the framework of our study, a change in the polymer segmental mobility can hardly been invoked to explain the accelerated aging behavior of the composite materials relative to neat PMMA. The absence of any shift in the calorimetric T_g associated with the equality for all the samples of the structural parameters issued from the modeling of the aging behavior to TNM model, provide strong evidence of similar dynamics among the samples of neat PMMA and PMMA/silica nanocomposites. Thus, the acceleration of the physical aging rate of PMMA in presence of silica particles does not seem to be linked to any change in the polymer dynamics.

Table 3. Diffusion Coefficient Values Obtained from Enthalpy Relaxation (DSC) and from Dielectric Permittivity (BDS) Measurements,[40] Related to the Characteristics of the Samples[a]

sample	area to volume ratio A/V (nm^{-1})	diffusion coefficient, D, at 80 °C (DSC) ($cm^2\ s^{-1}$)	diffusion coefficient, D, at 80 °C (BDS) ($cm^2\ s^{-1}$)
PMMA	3.1×10^{-4} [b]	5.16×10^{-13}	5.03×10^{-13}
A10	8.0×10^{-4}	5.83×10^{-13}	5.29×10^{-13}
R10	8.0×10^{-4}	5.12×10^{-13}	5.71×10^{-13}
V10	1.4×10^{-3}	4.43×10^{-13}	5.76×10^{-13}

[a] The values from BDS measurements are recalculated employing a corrected value of the dielectric strength of PMMA β process at infinite time (see text). [b] The A/V in bulk PMMA is determined assuming the presence of an internal length scale. For details, see ref 40.

Our study pointed out that the physical aging rate is rather related to the ratio of the area of silica to the volume of PMMA, which is also linked to the interparticle distance of silica in PMMA. It is therefore interesting to compare our results with studies reporting on the physical aging behavior of polymer thin films, considered as model systems for nanocomposites for which the thickness of the film is related to the average interparticle distance of nanoparticles in a polymer matrix[81,83] and also with the studies carried out on other confined systems like polymers in nanopores.[9] Most of these studies report a reduction or a suppression of the physical aging when the confinement length scale, i.e., the thickness of the polymer film, decreases.[10,11,28] Generally, the reduction of the physical aging rate is deduced from the reduction in the development of aging overshoot curves while its suppression is deduced from the absence of overshoot curves in calorimetric and volumetric studies of physical aging.[28] This reduction in the development of the overshoot curves in comparison with the bulk is also observed in our composites samples and also in agreement with the experimental results of Amanuel et al. for PVAc containing silica particles,[15] those of Nutt et al. for epoxy/clay nanocomposites,[14] those of Brinson et al. for PMMA/SWCNT,[82] and finally those of Simon et al. for OTP confined in nanopores,[9] for which the magnitude of the endothermic overshoot decreased with the increase of the ratio area of fillers/volume of polymer in the case of nanocomposites and with the decrease of the confinement length scale in the case of OTP in nanopores. Nevertheless, one has to be careful in the interpretation of such a reduction of the endothermic overshoot, which may be misleading. Indeed, it is important to highlight several points revealed by our study: (i) for the shortest aging times (less than 6 h), the development of the endothermic overshoot is more important for the composite sample with the highest ratio of area of silica/volume of PMMA; (ii) the composite samples reach the plateau value of enthalpy recovery at shorter aging times than neat PMMA; (iii) the total amount of recovered enthalpy is smaller (~10%) in the composite samples (see Table 1). The direct comparison of the magnitude of the endothermic overshoots among the different samples thus appears to be not so rigorous. This has been shown in our study by the use of a relaxation function taking into account the total amount of recovered enthalpy to quantify the physical aging behavior: even if the direct comparison of the DSC curves obtained after annealing shows an apparent reduction of the

physical aging, the plots of the relaxation function bring strong evidence of an acceleration of the physical aging in the composite samples, in accordance with the appearance of endothermic overshoots for very short aging times in these samples. In a forthcoming publication, we will show that indeed the initial value of the enthalpy could already correspond to a partially relaxed structure of the polymer in the nanocomposite. This provides an explanation to the relatively smaller value of the recovered enthalpy in the nanocomposites in comparison to pure PMMA (reported in Table 1). Therefore, the suppression of physical aging reported in some studies for the shortest confinement length scales in the case of thin films,[11,28] or for the shortest interparticle distances for the polymer nanocomposite systems,[12,13,81] may only be apparent, and in fact may be the result of a very important acceleration of the aging process, making it difficult to be detected in the studied temperature range and time scale, because aging already occurred before the beginning of the measurement. In particular, this would explain the recent results by Rowe et al.[84] who, measuring the permeability in several ultrathin glassy polymer films (less than 50 nm), showed a slower time evolution of the permeability for the thinnest films, also displaying a significantly smaller initial value of the permeability than the "bulk". Indeed, this lower initial value of the permeability for the thinnest films with respect to the bulk suggests that this value does not correspond to the unaged state of the polymer (at $t_a = 0$), but rather corresponds to a state at which the physical aging has already produced a decrease in the permeability through the induced densification of the polymer. This occurrence has been schematically sketched in our previous work.[40] This hypothesis is also in agreement with several studies reporting on the acceleration of physical aging in polymer films with thickness in the micrometer scale, with the decrease of the films thickness down to several hundreds nanometers.[8,20,21,24,26,36,37,84] In these cases, as in our study, the acceleration of the physical aging is limited enough to be detected by the used measurement techniques in the studied temperature ranges and time scales. Moreover, the physical aging of these systems has also been successfully described hypothesizing the diffusion of free volume holes toward the external surface.[20,21,37−39,77]

In the case of the present study, as well as in other PMMA/silica systems, an alternative explanation for the reduced recovered enthalpy or, in the case of the works presented in the literature the suppression of physical aging, would be that of strong hydrogen bonding between PMMA and silica.[10,12] However, in our view this explanation fails to explain the invariance of PMMA segmental dynamics after the introduction of silica nanoparticle found in our nanocomposites samples.[40] Furthermore, as previously discussed, a reduction of the "apparent" rate of physical aging has also been observed by Rowe et al.[84] in free-standing polymer films where no interfacial interaction can be invoked to explain such a reduction.

Summary and Conclusions

The effects of the presence of silica particles on the glass transition of PMMA and its structural recovery were investigated by DSC. Measurements of the enthalpy recovery were made as a function of aging time at the aging temperature of 80 °C. The comparison of the endothermic overshoot obtained for PMMA and for its composites showed that (i) at very short aging times, the endothermic overshoot is significantly larger for the nanocomposites; (ii) at very long aging times, the endothermic overshoot is reduced but broader for the nanocomposites relative to neat PMMA; and (iii) the composite samples reach the plateau value at shorter aging times than neat PMMA. These results show that the aging kinetics of PMMA is affected by the presence of silica particles, despite the lack of effect of the particles on the glass transition temperature and in general the segmental dynamics.

The comparison of the physical aging rate of PMMA and PMMA/silica composites was carried out by means of a relaxation function, in order to take into account the different total amounts of recovered enthalpy among the different samples. The use of this relaxation function brought strong evidence of an acceleration of the physical aging of PMMA in presence of silica particles. Moreover, it was also found that the higher the ratio area of silica/volume of PMMA in the composites, the faster the physical aging of PMMA in the sample, whereas the shape of the relaxation functions remains unaltered.

The results were then successfully described by means of the TNM phenomenological model, widely accepted to describe the structural relaxation of glasses. The fitting to TNM model gave rise to equal structural parameters (β, x, Δh) for all the samples. These results indicate that the molecular mechanism for physical aging in PMMA is not affected by the presence of silica particles. The only different fitting parameter accounting for the difference in physical aging rates among the samples was found to be the pre-exponential factor, dependent on the area/volume ratio of silica in the polymer. These findings well agree with recent results obtained on the same nanocomposites monitoring the physical aging by means of BDS. This observation can be rationalized considering that the physical aging process is driven by the diffusion of free volume holes toward polymer interfaces. This hypothesis was verified by the successful calculation of physically meaningful diffusion coefficients of free volume holes in PMMA and its nanocomposites, according to a model of diffusion of free volume holes.

Acknowledgment. The authors acknowledge the University of the Basque Country and Basque Country Government (Ref. No. IT-436- 07, Depto. Educación, Universidades e Investigación, and iNANOGUNE research project within Etortek program) and the Spanish Minister of Education (Grant No. MAT 2007-63681) for their support. The support of the European Community within the SOFTCOMP program is also acknowledged. The SGIker UPV/EHU is acknowledged for the electron microscopy facilities of the Gipuzkoa unit. Juan González-Irun and Luis M. Liz-Marzan, from the department of Physical Chemistry of the University of Vigo (Spain), are gratefully acknowledged for the samples preparation.

References and Notes

(1) Hussain, F.; Hojjati, M.; Okamoto, M.; Gorga, R. *J. Compos. Mater*. **2006**, *40*, 1511–1575.
(2) Blond, D.; Barron, V.; Ruether, M.; Ryan, K.; Nicolosi, V.; Blau, W.; Coleman, J. *Adv. Funct. Mater*. **2006**, *16*, 1608–1614.
(3) Coleman, J.; Cadeck, M.; Ryan, K.; Fonseca, A.; Nagy, J.; Blau, W.; Ferreira, M. *Polymer* **2006**, *47*, 8556–8561.
(4) Ash, B.; Siegel, R.; Schadler, L. *Macromolecules* **2004**, *37*, 1358–1369.
(5) Struik, L. C. E. *Physical aging in amorphous polymers and other materials*; Elsevier: Amsterdam, 1978.
(6) Kovacs, A. J.; Aklonis, J. J.; Hutchinson, J. M.; Ramos, A. R. *J. Polym. Sci., Polym. Phys*. **1979**, *17*, 1097–1162.
(7) Priestley, R. D. *Soft Matter* **2009**, *5*, 919–926.
(8) Huang, Y.; Paul, D. R. *Polymer* **2004**, *45*, 8377–8393.
(9) Simon, S. L.; Park, J. Y.; McKenna, G. B. *Eur. Phys. J. E* **2002**, *8*, 209–216.
(10) Priestley, R. D.; Broadbelt, L. J.; Torkelson, J. M. *Macromolecules* **2005**, *38*, 654–657.
(11) Priestley, R. D.; Ellison, C. J.; Broadbelt, L. J.; Torkelson, J. M. *Science* **2005**, *309*, 456–459.
(12) Priestley, R. D.; Rittigstein, P.; Broadbelt, L. J.; Fukao, K.; Torkelson, J. M. *J. Phys.: Condens. Matter* **2007**, *19*, 205120.
(13) Rittigstein, P.; Torkelson, J. M. *J. Polym. Sci. B: Polym. Phys*. **2006**, *44*, 2935–2943.
(14) Lu, H.; Nutt, S. *Macromol. Chem. Phys*. **2003**, *204*, 1832–1841.

(15) Amanuel, S.; Gaudette, A. N.; Sternstein *J. Polym. Sci., B: Polym. Phys.* **2008**, *46*, 2733–2740.
(16) Vlasveld, D. P. N.; Bersee, H. E. N.; Picken, S. J. *Polymer* **2005**, *46*, 12539–12545.
(17) Huang, Y.; Paul, D. R. *Macromolecules* **2006**, *39*, 1554–1559.
(18) Fukao, K.; Sakamoto, A. *Phys. Rev. E* **2005**, *71*, 041803.
(19) Lu, H.; Nutt, S. *Macromolecules* **2003**, *36*, 4010–4016.
(20) Cangialosi, D.; Wubbenhorst, M.; Groenewold, J.; Mendes, E.; Schut, H.; van Veen, A.; Picken, S. J. *Phys. Rev. B* **2004**, *70*, 224213.
(21) Cangialosi, D.; Wubbenhorst, M.; Groenewold, J.; Mendes, E.; Picken, S. J. *J. Non-Cryst. Solids* **2005**, *351*, 2605–2610.
(22) Richardson, H.; Carelli, C.; Sferrazza, M.; Keddie, J. L. *Eur. Phys. J. E* **2003**, *12*, 437–441.
(23) Richardson, H.; Lopez-Garcia, I.; Sferrazza, M.; Keddie, J. L. *Phys. Rev. E* **2004**, *70*, 051805.
(24) Dorkenoo, K.; Pfromm, P. H. *Macromolecules* **2000**, *33*, 3747–3751.
(25) Wong, C. C.; Qin, Z.; Yang, Z. *Eur. Phys. J. E* **2008**, *25*, 291–298.
(26) Punsalan, D.; Koros, W. J. *Polymer* **2005**, *46*, 10214–10220.
(27) Zhou, C.; Chung, T. S.; Wang, R.; Goh, S. H. *J. Appl. Polym. Sci.* **2004**, *92*, 1758–1764.
(28) Kawana, S.; Jones, R. A. L. *Eur. Phys. J. E* **2003**, *10*, 223–230.
(29) Adam, G.; Gibbs, J. H. *J. Chem. Phys.* **1965**, *43*, 139–146.
(30) Donth, E.; Hempel, E.; Schick, C. J. *J. Phys: Cond. Matter* **2000**, *12*, L281–L286.
(31) Cangialosi, D.; Alegría, A.; Colmenero, J. *Phys. Rev. E* **2007**, *75*, 011514.
(32) Karmakara, S.; Dasguptaa, C.; Sastry, S. *Proc. Natl. Acad. Sci. U. S.A.* **2009**, *106*, 3675–3679.
(33) Scheidler, P.; Kob, W.; Binder, K. *Europhys. Lett.* **2002**, *59*, 701–707.
(34) He, F.; Wang, L. M.; Richert, R. *Phys. Rev. B* **2005**, *71*, 144205.
(35) Pfromm, P. H.; Koros, W. J. *Polymer* **1995**, *36*, 2379–2387.
(36) Dorkenoo, K. D.; Pfromm, P. H. *J. Polym. Sci., Polym. Phys.* **1999**, *37*, 2239–2251.
(37) McCaig, M. S.; Paul, D. R. *Polymer* **2000**, *41*, 629–637.
(38) McCaig, M. S.; Paul, D. R.; Barlow, J. W. *Polymer* **2000**, *41*, 639–648.
(39) Thornton, A. W.; Nairn, K. M.; Hill, A. J.; Hill, J. M.; Huang, Y. *J. Membr. Sci.* **2009**, *338*, 38–42.
(40) Boucher, V. M.; Cangialosi, D.; Alegría, A.; Colmenero, J.; González-Irun, J.; Liz-Marzan, L. M. *Soft Matter* **2010**, *6*, 3306–3317.
(41) Bogush, G. H.; Tracy, M. A.; Zukoski, C. F. *J. Non-Cryst. Solids* **1988**, *104*, 95–106.
(42) Hodge, I. M. *J. Non-Cryst. Solids* **1994**, *169*, 211–266.
(43) Mundra, M. K.; Donthu, S. K.; Dravid, V. P.; Torkelson, J. M. *Nano Lett.* **2007**, *3*, 713–718.
(44) Sargysan, A.; Tonoyan, A.; Davtyan, S.; Schick, C. *Eur. Pol. J.* **2007**, *43*, 3113–3127.
(45) Hub, C.; Harton, S. E.; Hunt, M. A.; Fink, R.; Ade, H. *J. Polym. Sci., B: Polym. Phys.* **2007**, *45*, 2270–2276.
(46) The fictive temperature is a measure of the instantaneous equilibrium configuration of a liquid. Below T_g, T_f represents the temperature at which a glass with a specific structure would be in equilibrium.
(47) Muzeau, E.; Vigiert, G.; Vassoille, R.; Perez, J. *Polymer* **1995**, *36*, 611–620.
(48) Borde, B.; Bizot, H.; Vigier, G.; Buleon, A. *Carbohydr. Polym.* **2002**, *48*, 111–123.
(49) Andreozzi, L.; Faetti, M.; Giordano, M.; Palazzuoli, D.; Zulli, F. *Macromolecules* **2003**, *36*, 7379–7387.
(50) Andreozzi, L.; Faetti, M.; Giordano, M.; Zulli, F. *Macromolecules* **2005**, *38*, 6056–6067.
(51) Alves, N. M.; Gomez Ribelles, J. L.; Mano, J. F. *Polymer* **2005**, *46*, 491–504.
(52) Andreozzi, L.; Faetti, M.; Giordano, M.; Palazzuoli, D. *J. Non-Cryst. Solids* **2003**, *332*, 229–241.
(53) Richardson, M. J.; Savill, N. G. *Polymer* **1975**, *16*, 753–757.
(54) Cowie, J. M. G.; Ferguson, R. *Polymer* **1993**, *34*, 2135–2141.
(55) Cowie, J. M. G.; Harris, S.; McEwen, I. J. J. *J. Polym. Sci., Part B: Polym. Phys.* **1997**, *35*, 1107–1116.
(56) Meseguer-Dueñas, J. M.; Garayo, A. V.; Romero Colomer, F.; Estellés, J. M.; Gómez Ribelles, J. L.; Monleón Pradas, M. J. *J. Polym. Sci., Part B: Polym. Phys.* **1997**, *35*, 2201–2217.
(57) Brunacci, A.; Cowie, J. M. G.; Ferguson, R.; McEwen, I. J. *Polymer* **1997**, *38*, 865–870.
(58) Pyda, M.; Wunderlich, B. *J. Polym. Sci., Part B: Polym. Phys.* **2002**, *40*, 1245–1253.
(59) Scherer, G. W. *J. Am. Ceram. Soc.* **1986**, *69*, 374–381.
(60) Narayanaswamy, O. S. *J. Am. Ceram. Soc.* **1971**, *54*, 491–498.
(61) Boucher, V. M.; Cangialosi, D.; Alegría, A.; Colmenero, J. *AIP Conf. Proc.* **2010**, *1255*, 172–174.
(62) Ferry, J. D. *Viscoelastic Properties of Polymers*; Wiley: New York, 1980.
(63) Moynihan, C. T.; Macedo, P. B.; Montrose, C. J.; Gupta, P. K.; DeBolt, M. A.; Dill, J. F.; Dom, B. E.; Drake, P. W.; Easteal, A. J.; Elterman, P. B.; Moeller, R. P.; Sasabe, H.; Wilder, J. A. *Ann. N.Y. Acad. Sci.* **1976**, *279*, 15–35.
(64) Tool, A. Q. *J. Am. Ceram. Soc.* **1946**, *29*, 240–253.
(65) Mijovic, J.; Nicolais, L.; D'Amore, A.; Kenny, J. M. *Polym. Eng. Sci.* **1994**, *34*, 381–389.
(66) Hodge, I. M.; Berens, A. R. *Macromolecules* **1982**, *15*, 762–770.
(67) Privalko, V. P.; Demchenko, S. S.; Lipatov, Y. S. *Macromolecules* **1986**, *19*, 901–904.
(68) Hofer, K.; Mayer, E.; Hodge, I. M. *J. Non-Cryst. Solids* **1992**, *139*, 78–85.
(69) Hammond, V. H.; Houtz, M. D.; O'Reilly, J. M. *J. Non-Cryst. Solids* **2003**, *325*, 179–186.
(70) Simon, S. L.; Sobieski, J. W.; Plazek, D. J. *Polymer* **2001**, *42*, 2555–2567.
(71) O'Reilly, J. M. *J. Polym. Sci., Part B: Polym. Phys.* **2000**, *38*, 495–499.
(72) Badrinarayanan, P.; Zheng, W.; Li, Q. X.; Simon, S. L. *J. Non-Cryst. Solids* **2007**, *353*, 2603–2612.
(73) O'Reilly, J. M. *Crit. Rev. Solid State Mater. Sci.* **1987**, *13*, 259–277.
(74) Hutchinson, J. M. *Prog. Polym. Sci.* **1995**, *20*, 703–760.
(75) The physical aging is faster in the nanocomposite sample V10.
(76) Hodge, I. M. *J. Res. Natl. Inst. Stand. Technol.* **1997**, *102*, 195–205.
(77) Cangialosi, D.; Wubbenhorst, M.; Schut, H.; van Veen, A.; Picken, S. J. *Phys. Rev. B* **2004**, *69*, 134206.
(78) Chen, K.; Vyazovkin, S. *J. Phys. Chem. B* **2009**, *113*, 4631–4635.
(79) Nemilov, S. V.; Johari, G. P. *Philos. Mag.* **2003**, *27*, 3117–3132.
(80) Hu, L.; Yue, Y. *J. Phys. Chem. B* **2008**, *112*, 9053–9057.
(81) Rittigstein, P.; Priestley, R. D.; Broadbelt, L. J.; Torkelson, J. M. *Nat. Mater.* **2007**, *6*, 278–282.
(82) Flory, A. L.; Ramanathan, T.; Brinson, C. L. *Macromolecules* **2010**, *43*, 4247–4252.
(83) Bansal, A.; Yang, H.; Li, C.; Cho, K.; Benicewicz, B. C.; Kumar, S. K.; Schadler, L. S. *Nat. Mater.* **2005**, *4*, 693–698.
(84) Rowe, B. W.; Freeman, B. D.; Paul, D. R. *Polymer* **2009**, *50*, 6149–6156.